IMPROVING THE ENERGY EFFICIENCY OF WIRELESS SENSORS THROUGH SMART ANTENNA DESIGN

A. Mason, A. Shaw, A. I. Al-Shamma'a
Liverpool John Moores University,
Liverpool, United Kingdom.

ABSTRACT

There is a growing trend in the use of intelligent Wireless Sensor Networks (WSNs) for a wide range of applications. In the early part of the decade the underlying hardware was largely in prototype form and used for small scale demonstration systems, but there is now growing interest in applications which are commercially viable. This work began on the premise that the sensor hardware has gradually become smaller, yet there are still a few peripheral components which are lagging behind; namely the battery and antenna. Here, a novel antenna design is presented; this antenna is of a practical size for use in WSNs, whilst also offering improved energy consumption over commonly used monopole antennas.

1. INTRODUCTION

Antennas are critical to the operation of wireless communication systems such as those used for radio, television, and mobile phones. They are often taken for granted by an end user of such a product – many consumers are blissfully unaware of how much antenna design can impact on device performance, size and energy consumption. Antenna design is often forgotten in WSNs since the devices are deployed in close proximity to one another (i.e. with a separation of 10m or less). As a result, device communication with simple wire antennas is a simple and affordable solution, but is not necessarily efficient. This leads to data corruption during wireless transmission which can result in three possible scenarios:

- ***Loss;*** the data is irreparable and is lost forever – in this case the energy put into capturing, processing and transmitting the data is wasted.
- ***Recovery;*** some protocols may allow data recovery, implying that there is a permanent data overhead which incurs additional energy consumption.
- ***Retransmission;*** important data may be repeatedly transmitted until the intended message is correctly received – this ensures reliability, but leads to wasted energy.

Therefore, it is desirable to have a system which minimises data corruption in order to improve efficiency, particularly when one takes into account the fact that data transmission from a typical sensor node consumes three times more energy than data processing alone [1].

In addition to the energy problem, the physical form of the standard monopole antenna is considered to be unsuitable for many applications. In particular the authors have been

involved in the use of WSNs for inventory management [2, 3] and spot weld monitoring [4]. In these situations it is undesirable for the sensor node, or mote, antenna to protrude from the object to which it is attached, since both applications involve high speed movement which could damage or destroy the antenna should it be snagged.

The devices used as part of the authors work are the commonly known MicaZ motes [1], one of which is shown in Figure 1. One can clearly see here that the monopole antenna protrudes some way from the mote; the length of the protrusion is linked to the operating frequency of the mote, and therefore its wavelength (λ) [5]. In this case the operating frequency is 2.45GHz, and λ = 122mm. Monopole antennas are typically λ/4 in length [6] and there is no exception here as the MicaZ antenna measures approximately 40mm*. The initial thought in this situation was to simply flatten the antenna and effectively shield it from damage. This scenario is shown clearly in Figure 2.

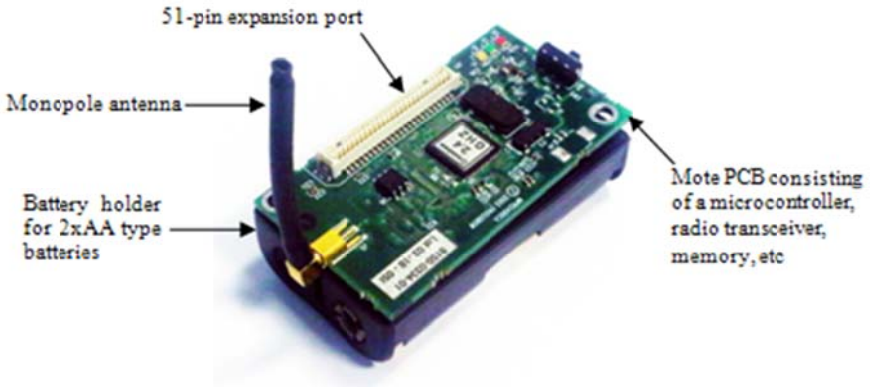

Figure 1. Berkeley MicaZ mote with monopole antenna attached.

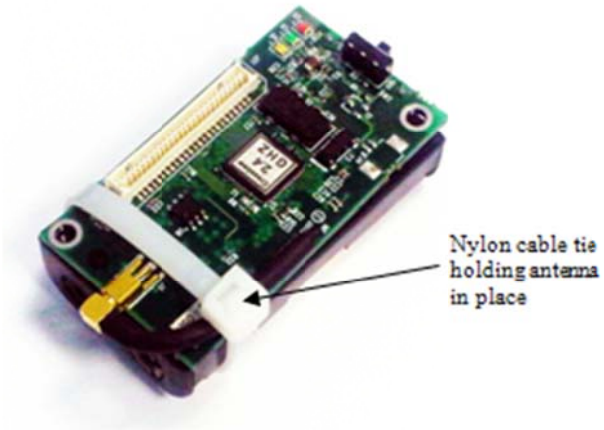

Figure 2. Mote antenna held in place with a nylon cable tie to prevent snagging.

* Note that λ/4 = 31mm at 2.45GHz, but the MicaZ antenna includes a sheath which is slightly longer than the antenna so as to offer limited protection.

A simple experiment, using one mote as a transmitter and another as a receiver, demonstrated that flattening the antenna caused significant signal strength degradation. When the transmitter and receiver are separated by 1m of air, the signal strength was found to be 10dBm less if the antenna was flattened, compared to if the antenna was in its normal position (see Figure 1). As a result of these findings it was thought that designing a new antenna for the motes might be a more effective solution, since significant losses in signal strength ultimately lead to data loss.

2. DESIGNING A NEW ANTENNA

2.1. ANTENNA REQUIREMENTS

Since industry disliked the idea of the existing MicaZ monopole antenna alternative types were considered. Wire antennas such as dipoles are typically in the order of $\lambda/2$ in length, and loop antennas often have a circumference equal to λ. We can see that dipole and loop antennas would be larger than the standard monopole antenna supplied with the MicaZ and therefore likely to be an even greater concern for industrial use. Smaller sizes are possible for loops and dipoles, but they do not make effective radiators [7, 8].

The best remaining option was a PCB antenna. With size and practicality being major concerns of industry it seemed that a low profile PCB antenna would be ideal. It was thought that such an antenna would be suitable for retrofitting to the current MicaZ motes, and in the future could possibly be integrated with the mote circuitry in a combined PCB design. In order to facilitate this, an aim was set of creating an antenna no greater than the size of MicaZ PCB (i.e. - 57mm × 32mm).

Although PCB antennas do have their advantages, it is noted in literature that they tend to suffer from a narrow impedance bandwidth, quite often in the order of just a few percent [5]. The impedance bandwidth [9] refers to the ability of an object to absorb or transmit energy into its surroundings; in the case of antennas, the later is desirable. Impedance bandwidth can be calculated using Equation 1, where f_u is the upper operating frequency, f_l is the lower operating frequency and f_0 is the centre frequency. f_u and f_l refer to the points where the energy transmitted by an antenna is ≥ 88.9%. In some texts this is also referred to as the point where the voltage standing wave ratio (VSWR) is ≤ 2 [10], and describes the range over which antennas are effective radiators.

$$Bandwidth(\%) = \left(\frac{f_u - f_l}{f_0} \right) \times 100 \qquad \text{(Equation 1)}$$

For the MicaZ mote, f_l = 2.485GHz, f_u = 2.400GHz and f_0 = 2.443GHz [1], since the devices support multiple frequency channels for reduced interference. These figures lead to a minimum impedance bandwidth requirement of 3.48%.

In addition to these requirements it was also thought that the antenna should have good directional properties (i.e. seek to radiate equally well in all directions). In literature this is often better defined as directivity, but this parameter is often difficult to quantify accurately, therefore this work takes a qualitative approach. Low directivity is critical for WSNs since it is often impossible to control the orientation of nodes during deployment – in mobile applications (e.g. inventory management) orientation may also vary significantly

with time. Antennas with only a single plane of polarisation cannot communicate well (if at all) with those orientated perpendicular to themselves [11]; monopole and dipole antennas suffer noticeably from this issue.

To summarise before continuing, the new antenna was required to:

- operate at the centre frequency (f_0) 2.443GHz.
- have an impedance bandwidth greater than 3.48%.
- be no larger than 57mm×32mm×1.6mm.
- have a low directivity.

2.2. COPLANAR WAVEGUIDE (CPW) ANTENNA

During a review of literature relating to antenna design, it was discovered that Nithisopa et al [12] had designed a broadband co-planar waveguide (CPW) fed slot antenna which, in simulations, had proven suitable for use over the range of approximately 2.35-2.70GHz, resulting in an impedance bandwidth of 14%.

The term CPW refers to the way in which the antenna is fed; two parallel slots are cut into a copper surface to act as a transmission line feed to the radiating elements of the antenna itself – this is illustrated in Figure 3. The radiating elements come in many different forms, although it appears that the slot type is popular. The copper surrounding the feed slots acts as a ground plane which promotes more uniform radiation than one would experience with similar structures such as patch antennas [5, 13, 14]. Based upon the work conducted by Nithisopa, an Ansoft HFSS [15] model was created as shown in Figure 3. The model was set up by following strict guidelines [16] provided by the developer of HFSS for the creation of CPW models. Table 1 gives information relating to the dimensions illustrated in Figure 3.

Dimensions *W1* and *W2* are of particular importance in impedance matching the antenna to a typical 50Ω transmission line. Impedance matching is vital in antenna design in order to ensure that as much power as possible from the radio transceiver is transferred to the propagation medium via the antenna [17]. Poor matching leads to power being reflected by the antenna back toward the transceiver, resulting in reduced transmission range, wasted energy and potential damage to the transceiver itself.

Figure 4 shows the difference in simulated performance as a result of using FR4 instead of Duroid substrate, as in Nithisopa's work. The reason for changing substrate was simply a case of using materials to hand at the time for prototype manufacture, but one can see that the increase in dielectric constant (ε_r) reduces the impedance bandwidth. For Duroid $\varepsilon_r \approx 2$, but for FR4 $\varepsilon_r \approx 4$. Despite the decrease in impedance bandwidth FR4 still resulted in an impedance bandwidth – calculated to be 10% – far exceeding the requirements for this application.

Table 1. CPW dimensions (mm).

h	*pcbX*	*pcbY*	*W1*	*W2*	*H1*	*H2*	*L1*
1.6	90.0	45.0	0.5	2.4	23.0	10.5	39.0

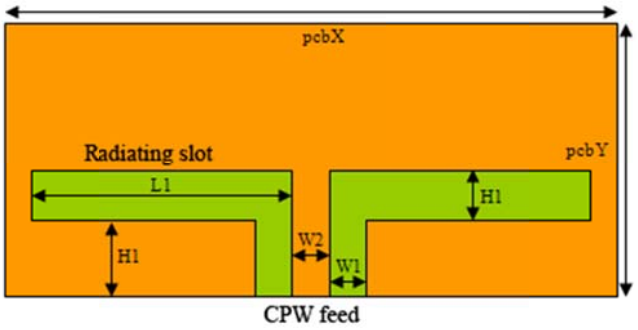

Figure 3. CPW antenna structure and dimensions.

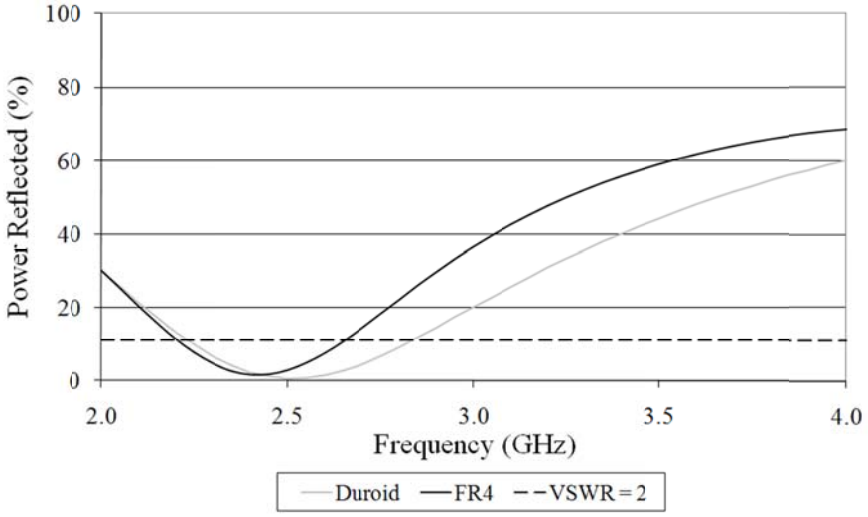

Figure 4. Simulated reflected power for FR4 and Duriod substrates.

Another interesting property of Nithisopa's CPW antenna was its low directivity which is a significant advantage of CPW design when one considers other types of PCB antenna. Balanis [18] gives a guide to constructing a simple patch antenna, a structure mentioned in passing earlier. This structure consists of a rectangular conductive patch above a larger conductive ground plane. The two conductive layers are separated by a dielectric substrate, as shown in Figure 5. A comparison of the CPW antenna and a patch antenna created using the Balanis guide shows that the CPW antenna has a favourable radiation pattern for applications requiring low directivity; this is evidenced in Figure 6. The *xz* and *yz* planes are of particular interest at the 180° position where the patch antenna experiences attenuation in the order of 20dB – this is a direct result of the ground plane preventing transmission in this direction. The downside for the CPW antenna is increased attenuation in the plane of the PCB when compared with the patch antenna. However this is a reasonable compromise as the loss is much smaller than that caused by the patch antenna ground plane.

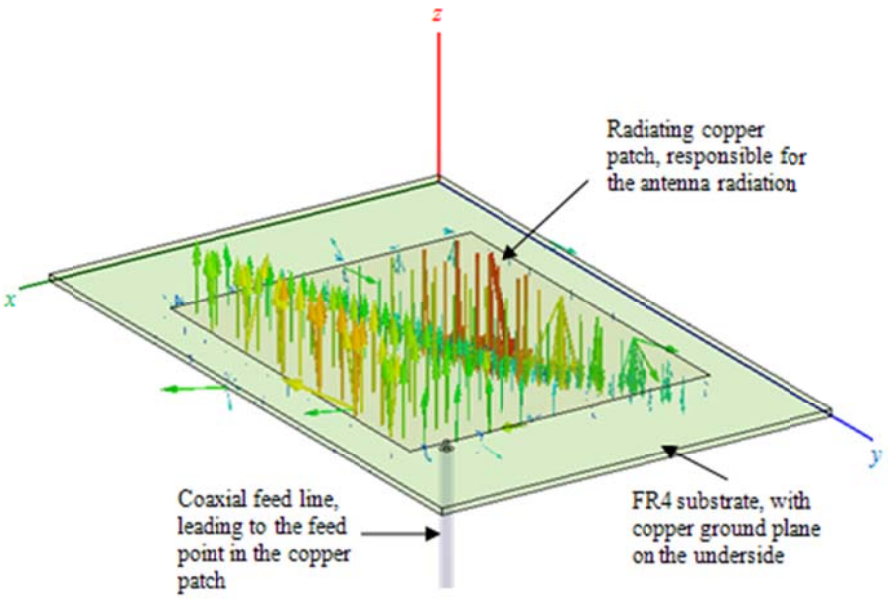

Figure 5. A simulated patch antenna, constructed using a guide by Balanis [18]. Note that the model is transparent so that the electric vector field is visible across the entire structure.

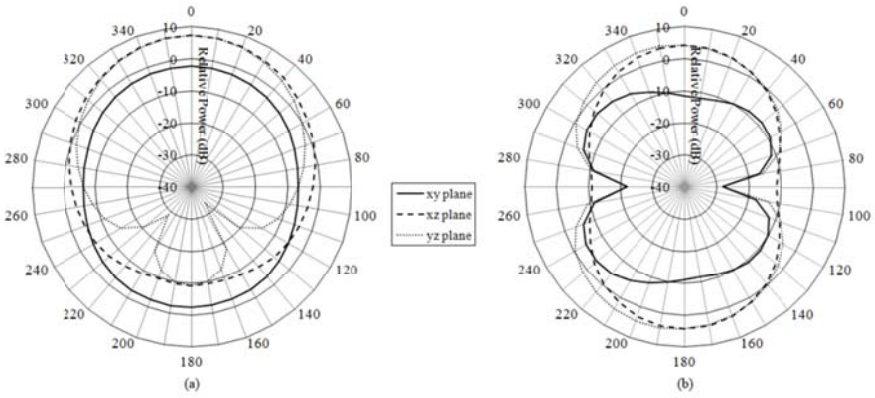

Figure 6. Simulated radiation patterns of the (a) patch and (b) CPW antennas.

Despite the CPW antenna providing a bandwidth much greater than that required and having low directivity, it was still too large. Therefore further investigation ensued with CPW antennas remaining the focus of attention.

2.3. FOLDED COPLANAR WAVEGUIDE (FCPW) ANTENNA

In order to solve the issue of size with the CPW antenna, the largest dimension (*pcbX*) was considered. This dimension had to accommodate the radiating slots of length *L1*, which were ultimately responsible for radiating power into the transmission medium (i.e. the surrounding air). Thinking of the slots as being analogous to the two arms of a standard wire dipole antenna, some thought was given to what might happen if the slots were folded, therefore allowing them to be accommodated by a shorter *pcbX* dimension. Folded wire dipole [19] antennas are created by taking the two radiating elements of a standard λ/2 dipole and folding them to form a closed loop; this transition is shown in Figure 7.

By applying a similar train of thought to the CPW antenna a new folded co-planar waveguide (FCPW) antenna was created. The simulation model for this antenna is shown in Figure 8, and Table 2 shows the dimensions used for this structure after applying parametric analysis to the model in order to optimise its radiation characteristics.

The simulated radiation pattern is shown in Figure 9, and is not too far removed from that of Nithisopa's CPW antenna. The simulated impedance bandwidth was calculated to be 61% - this is discussed further later.

Given the promising impedance bandwidth and directivity results, the largest improvement with the FCPW antenna, in terms of achieving the initial goals, was size reduction. The initial requirements, stated in Section 2.1, were 57mm×32mm×1.6mm. The FCPW antenna is 40mm×27.5mm×1.6mm. This gives a total surface area saving of 39.7%, indicating that the antenna could be suitable for WSN nodes smaller than the Berkeley MicaZ.

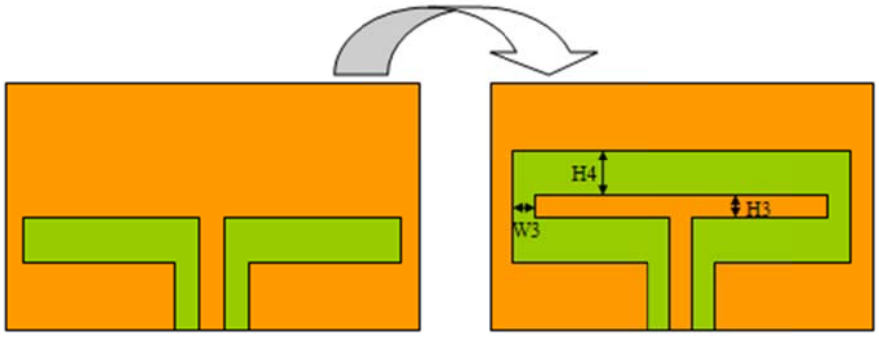

Figure 7. Converting the CPW antenna to a folded CPW antenna, with new dimensions also labelled.

Table 2. FCPW dimensions (mm).

h	pcbX	pcbY	W1	W2	W3	H1	H2	H3	H4	L1
1.6	40.0	27.5	0.5	4.0	1.5	2.0	4.0	0.5	8.5	39.0

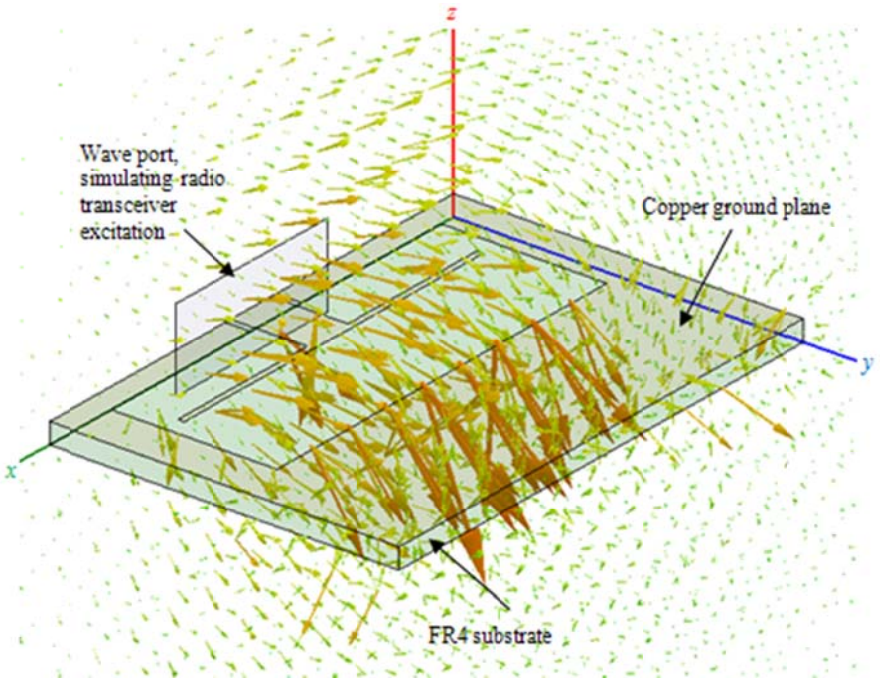

Figure 8. FCPW antenna simulation model, showing the electric vector field surrounding the antenna.

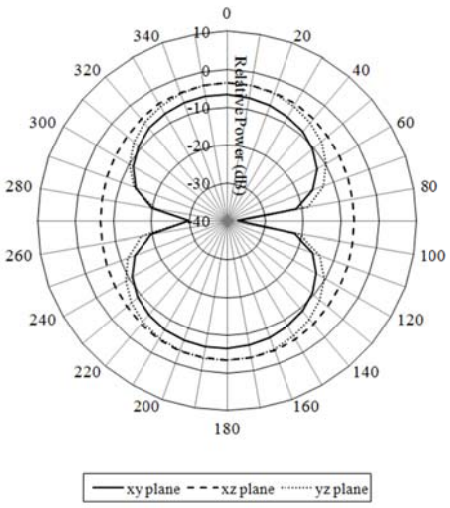

Figure 9. FCPW antenna simulated radiation pattern.

2.4. VALIDATING THE DESIGN

The prototype FCPW antenna is shown in Figure 10. It has a bulkhead type SMA connector attached so as to allow connection to various devices (including the Berkeley MicaZ via an inter-series MMCX to SMA adaptor). Use of an SMA connector was convenient for experimentation purposes, the results of which are presented in the next section. It is imagined that this connector would not be necessary if the antenna were used in practise – instead the antenna could be connected directly to the radio transceiver of a wireless sensor node. The centre conductor of the SMA connector is soldered to the centre copper strip, whilst the outer conductor is connected to the antenna ground plane on either side of the centre strip.

The simulated results for reflected power and those measured using the Anritsu VNA show a reasonable agreement (see Figure 11). At 2.45GHz the reflected power is just 2.6% - this means that 97.4% of the power incident to the antenna should be radiated. The impedance bandwidth during simulation was found to be 61%, whilst the measured bandwidth is 53%. This is more than adequate for the successful operation of the MicaZ mote over all of its selectable frequencies.

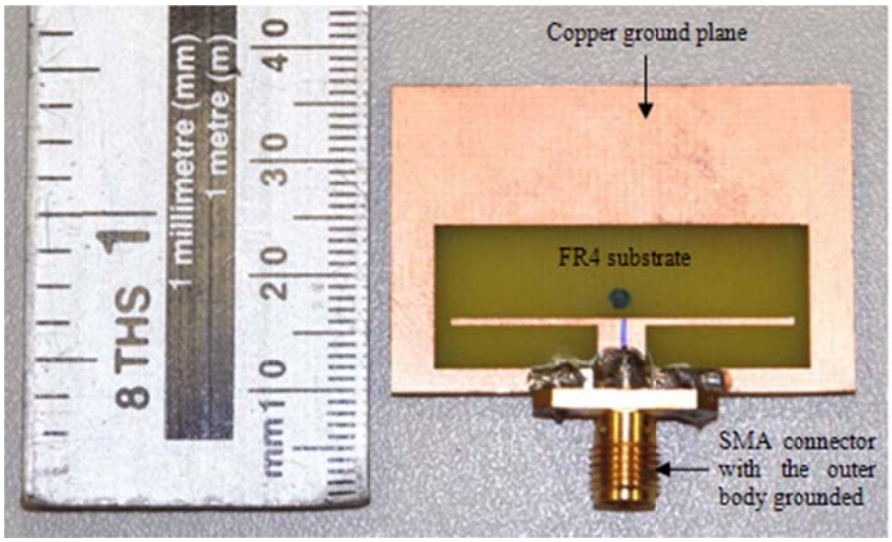

Figure 10. Prototype FCPW antenna post construction.

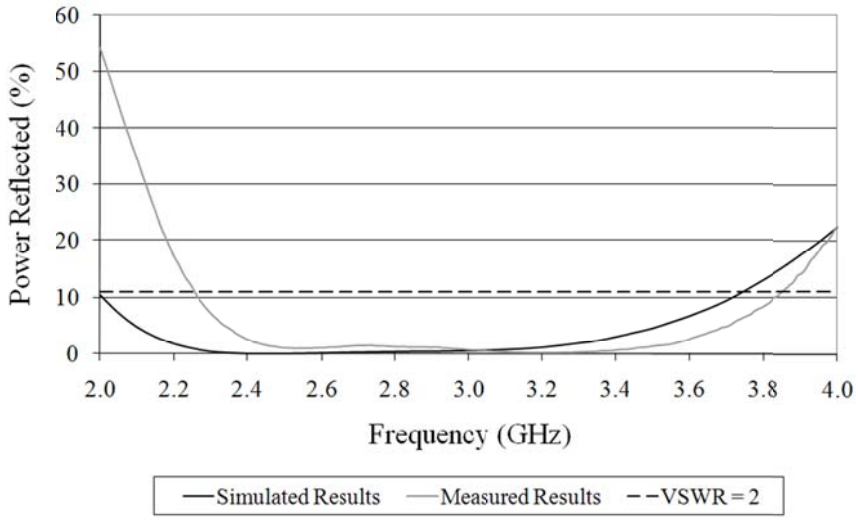

Figure 11. Simulated vs. measured reflected power for the FCPW antenna.

3. RADIATION PATTERN MEASUREMENT

3.1. METHODOLOGY

Simulations gave an indication of the FCPW antenna radiation pattern, however physical confirmation of this was required in order to validate the design. Testing antennas is not a trivial task as one must take a number of steps to ensure that measurements are not subject to interference from surrounding sources; this is particularly relevant here due to the wide range of uses for the ISM 2.4GHz frequency band (e.g. WLAN infrastructure).

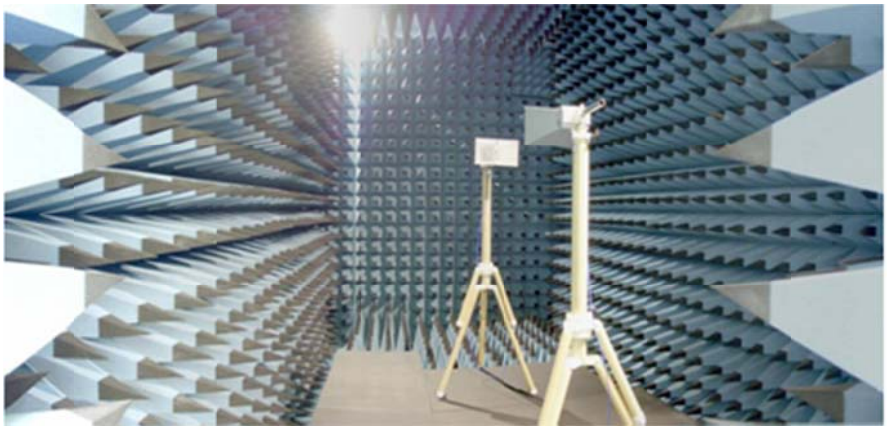

Figure 12. Inside a typical anechoic chamber.

Small antennas are typically tested in almost ideal conditions inside a structure known as an anechoic chamber [20]. Such chambers are usually shielded with a thick conducting metal, thus utilising the skin effect [21] to prevent signals from the outside world entering the chamber. An example of such a chamber is shown in Figure 12. Unfortunately, an anechoic chamber was not available for this work since they are costly to rent, and even more costly to build. Therefore an alternative method for testing was put into operation.

It was thought that since WLAN infrastructure is typically localised to urban areas in the UK, tests could be carried out in a rural scenario where interference would be reduced. In addition, it was thought that a rural location, such as a large open field, would allow transmitted signals to simply travel away from the antenna and into space. This avoids issues with electromagnetic phenomena such as multipath fading [22-24].

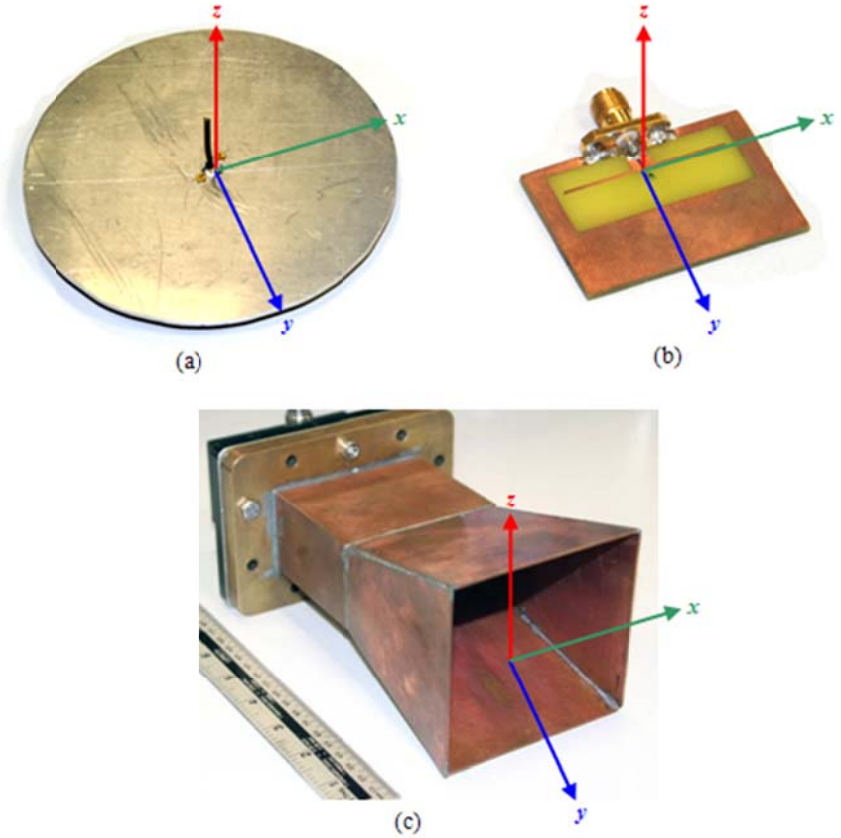

Figure 13. Antennas used for experimentation, including orientation indicators; (a) monopole (b) FCPW and (c) horn.

In addition to the FCPW antenna two further antennas were required; a reference (for comparison purposes), and a receiver. The reference antenna constructed was a λ/4 monopole with a ground plane, designed to approximate the performance of the default MicaZ monopole antenna. A horn antenna was chosen as the receiver since they are well known to have a high directivity [25] and are therefore unlikely to be affected by signals which originate from anywhere but directly in front of the horn aperture. In addition, horn antennas are highly orientation sensitive and only accept radiation in a single plane when they are used at their fundamental operating frequency. The chosen horn had dimensions appropriate for use at 2.4GHz. All three antennas are shown in Figure 13.

Both the receiver (horn) and transmitter (monopole or FCPW) needed to be suspended 1.5m above ground level in order to prevent reflections from the floor causing multipath interference. In order to do this, tripods were employed, as shown in Figure 14. The receiving horn antenna was bolted to the top of a large surveyor's tripod. Since it was assumed that the ground in a rural setting would not be particularly level, a base was made for this tripod with a large bolt at each corner allowing the base to be levelled – a plumb line hanging from the centre of the tripod was used for levelling. A standard camera tripod with full height adjustment was used to mount the transmitter. Much of the tripod was made out of plastic rather than metal which was considered to be useful in terms of reducing its impact on the experimental results (e.g. due to coupling). The mounting here was moveable through 360°, allowing rotation of the transmitting antenna in order to obtain radiation pattern measurements.

The two antennas were placed 1.5m apart to ensure that the measurements were in the antenna far field (as opposed to the near field). The far field of the monopole antenna is 0.276m, but Balanis [26] notes that this is not a fixed rule and so it seemed appropriate to allow additional range.

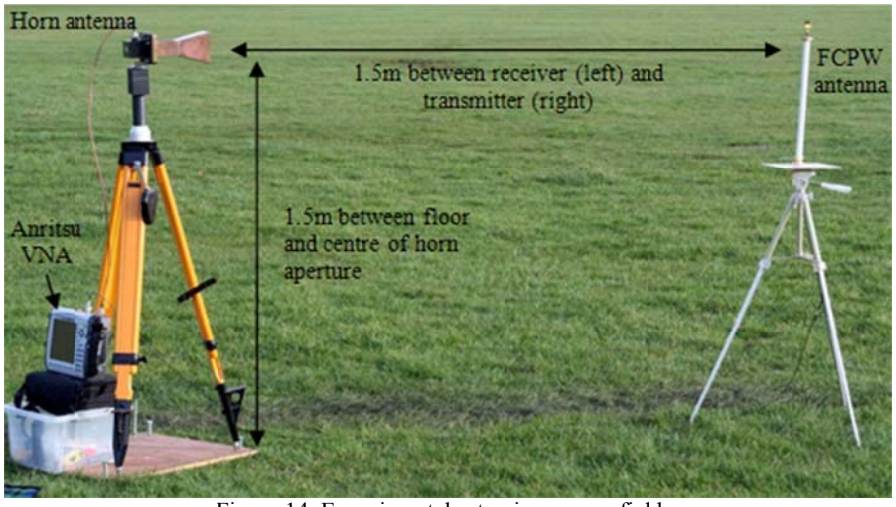

Figure 14. Experimental setup in an open field.

An Anritsu MS2024A vector network analyser (VNA) was used – the horn antenna was connected to its input port, and the transmitter to its output. The VNA was then used to measure the return loss†, in dB, at 2.45GHz. All measurements were repeated three times, and the averages used in the following sections; further repetitions were not practical because of changeable weather conditions and life time of the Anritsu VNA's battery.

3.2. MEASURED RADIATION PATTERNS

The results of these experiments represent the measured return loss arbitrarily normalised to -50dB. The measurements shown are relative to the antenna orientations indicated in Figure 13. For the monopole antenna the electric field is polarised in the *z* direction, whilst for the FCPW it is taken to be in the *y* direction. With the pyramidal horn being a flared waveguide, it is possible to assume [27] that the electric field is parallel to the *z* axis of the waveguide (see Figure 13). This means that turning the horn antenna through 90° allows one to consider how the antennas perform when there is a polarisation mismatch. The measurements shown in Figures 15 and 16 include the situation where the antennas polarisations are matched and mismatched respectively. This is important for this work since we cannot often guarantee the relative orientation of the antennas of sensor nodes in a WSN.

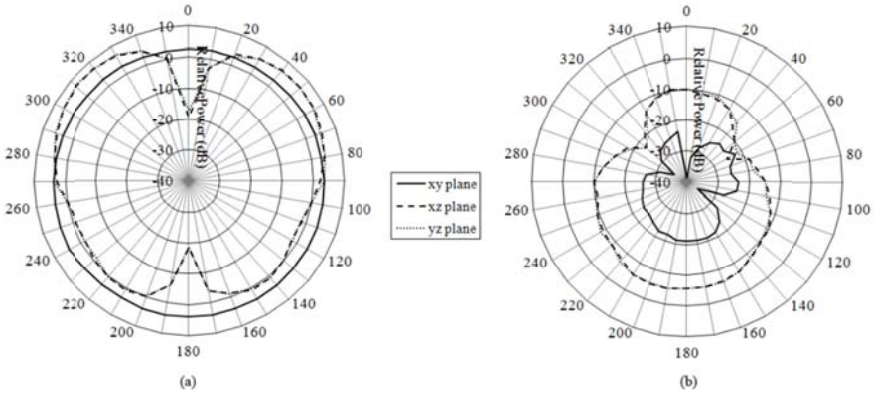

Figure 15. Monopole antenna radiation patterns with (a) matched and (b) mismatched polarisation.

† The ratio of received power (input) to transmitted power (output).

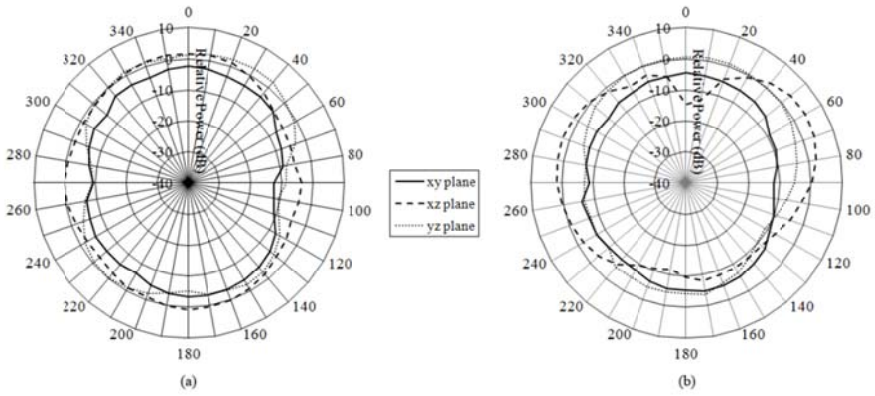

Figure 16. FCPW antenna radiation patterns with (a) matched and (b) mismatched polarisation.

3.3. DISCUSSION

Looking first at the results of the monopole antenna (Figure 15), we see good correlation of the measured radiation patterns with those from known and respected literature [28, 29]. This is an excellent indication of the validity of the measurement method used in this work.

When polarisation between the monopole and horn antennas is matched, as in Figure 15(a), we see in the *xy* plane that the monopole antenna acts isotropically; this is indicated by the reasonably uniform distribution of measured radiated power. However, in the *xz* and *yz* planes significant attenuation occurs in the *z* axis. Unlike infinite ground planes, their finite counterparts do not completely block transmission [13] but there is definite attenuation (in the order of 5-10dB) due to the presence of the monopole ground plane between 90° and 270° (not inclusive). The maximum measured power occurs in the *yz* plane at 310°, and is 8.07dB. The patterns are also generally quite symmetrical in the *z* axis, again as one would expect, so a similar peak can be found at 50°.

A wire antenna is said to have a polarisation which is parallel to the wire [11]. Therefore it is not surprising that, as shown in Figure 15(b), there is a significant loss experienced with the monopole antenna when polarisation is mismatched. This is particularly evident in the *xy* plane, where the radiated power reaches -40dB. There is some improvement in the *xz* and *yz* planes, although it is suspected that this is a result of reflections incident to the ground plane. It is possible that the ground plane is acting as a poor parabolic dish antenna in these cases.

Let us now consider the case of the FCPW antenna beginning with the radiation pattern results when polarisation is matched, as shown in Figure 16(a). Radiation is weakest in the plane of the PCB since electric field lines formed as a result of opposing charges on the FCPW ground plane converge at the PCB edges but cannot join. This is further highlighted in Figure 17. A drop in the radiated power of approximately 10dB is also present at the 90° and 270° degree positions due to the lack radiating elements covering these positions. Whilst a 10dB loss is significant, it is not nearly as significant as the loss that HFSS reported (shown as a 35dB loss in Figure 9). Another noteworthy feature is that the FCPW

antenna, whilst not outputting peak power near that of the monopole antenna, does not drop much below -10dB, whilst the monopole antenna drops to almost -20dB along the *z* axis.

Looking finally at the most exciting results from the FCPW antenna, shown in Figure 16(b), this antenna is much more tolerant of polarisation mismatch than the monopole antenna. In the *xy* plane there is typically a 2-3dB loss when compared with the monopole measurements shown in Figure 15(b); the same reductions in radiated power are present at the 90° and 270° positions. These reductions apply to the *yz* plane also. The most notable feature, however, is the *xz* plane which displays peaks of up to 4.05dB which is more than experienced by the antenna in the Figure 16(a).

So, the question is, why does the FCPW antenna exhibit such results? Looking at Figure 18 one can see that the vector fields radiate perpendicular to the PCB in most cases. A result of this is the drop in radiated power shown in Figure 16(b) in the *xz* plane at 0°, because directly above the antenna there is a polarisation mismatch, whilst there is an increase shown nearer the edges of the board. At the edges of the PCB the electric field appears to change direction so that it is nearly orthogonal to the field in the centre. This indicates that the polarisation of the electric field is not strictly linear, as is the case with the monopole antenna. Figure 19 serves to reinforce this argument. Here the electric field is shown to be parallel to the PCB; in the centre of the antenna the field is parallel to the *y* axis, but near the edges this changes and the field becomes almost parallel to the *x* axis.

The reason for this occurring is most likely due to the fold introduced to the antenna. Normally the electric field would form across the narrowest dimension of the radiating slots, but at the fold the electric field can form between the centre strip and the ground plane, opposing the direction of the central electric field. Since the results in Figure 16(a) and 16(b) are not identical (i.e. the two radiation patterns are not of the same magnitude) this indicates that the antenna has an elliptical rather than circular polarisation. This means that the antenna is not truly omni-directional, but does exhibit properties which are far more favourable than a simple monopole antenna. The next section of this chapter looks at the practical implications of these properties.

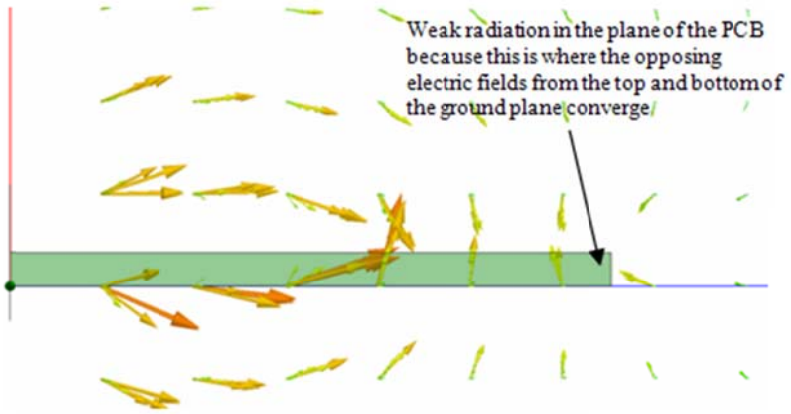

Figure 17. FCPW antenna simulated electric field vector plot showing the formation of fields at the edges of the PCB

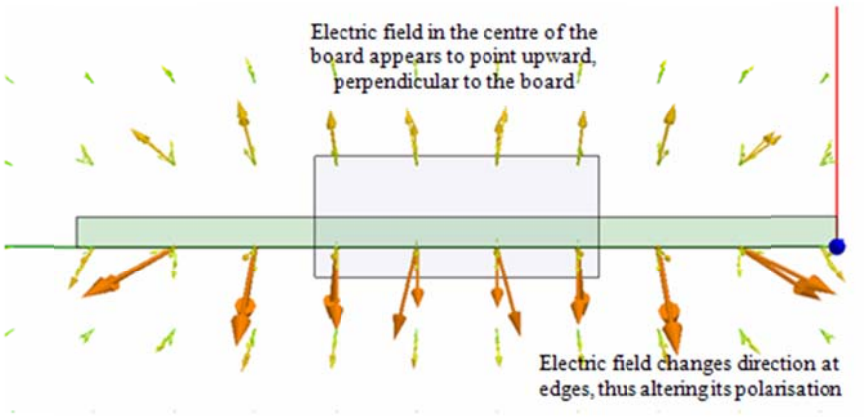

Figure 18. HFSS simulated vector field pattern for the FCPW antenna showing the formation of multiple polarisations (side view, *xz* plane)

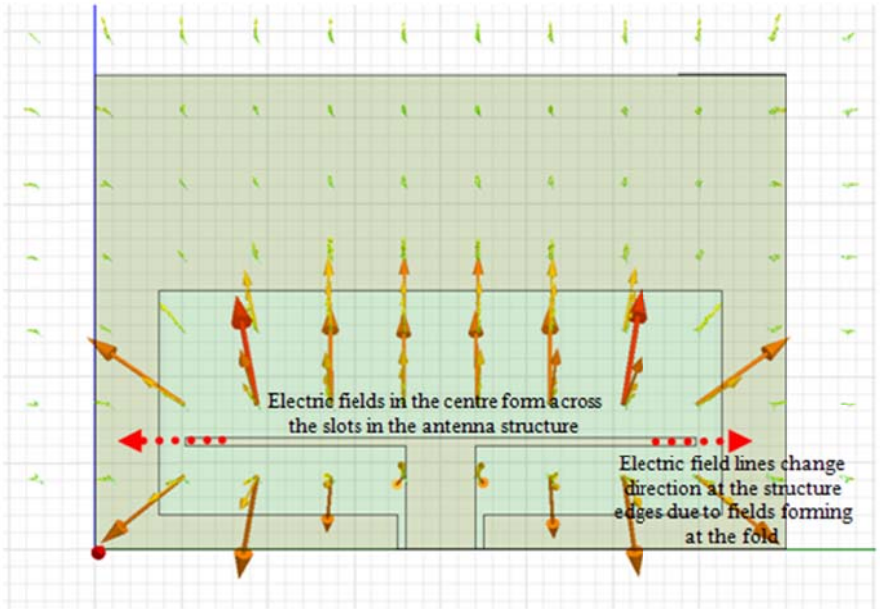

Figure 19. HFSS simulated vector field pattern for the FCPW antenna showing the formation of multiple polarisations (top view, *xy* plane)

4. ENERGY EFFICIENCY MEASUREMENTS

4.1. EXPERIMENTAL SETUP

Whilst a measurement of the antenna's radiation patterns was useful to understand how power was distributed around the FCPW antenna, it is important to highlight the real world implications of these measurements. Since the objective is to replace the MicaZ antenna, it was thought that this could involve a direct comparison of the existing monopole antenna and the FCPW antenna. Therefore experimental results were obtained which compared the two antennas in operation when attached to a MicaZ mote.

A PC application was written which utilised the Received Signal Strength Indicator (RSSI) feature of the motes to calculate a ten second average for signal strength, along with the number of data packets received (out of a maximum of 1000). It was decided to record both of these items of data to ensure not only a good signal strength, but also that data transmission was taking place. Figure 20 shows a screenshot of this application.

Tests were conducted outdoors, and the setup as shown in Figure 21. The base station and a moveable MicaZ node were placed 1.5m above ground level, and the distance between the two was then increased in 1m increments, starting at 0.1m and ending at 25m[‡]. The transmission power level of both the base station and the moveable node were set to 0dBm (i.e. 1mW). Various orientations of both the standard monopole and FCPW antenna were investigated, including what happened when a polarisation mismatch occurred.

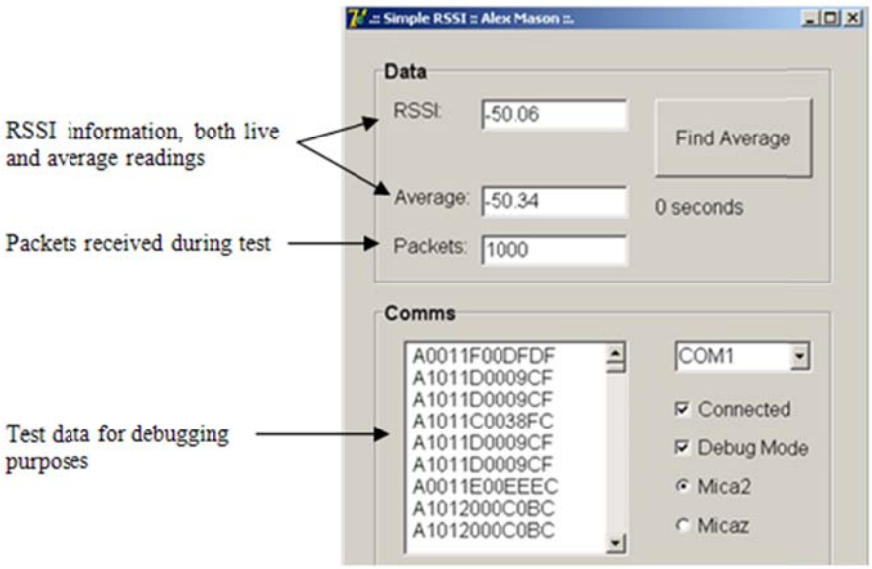

Figure 20. Bespoke application for recording mote RSSI and packet loss information.

[‡] The first interval was 0.9m in order to accommodate the 0.1m initial spacing.

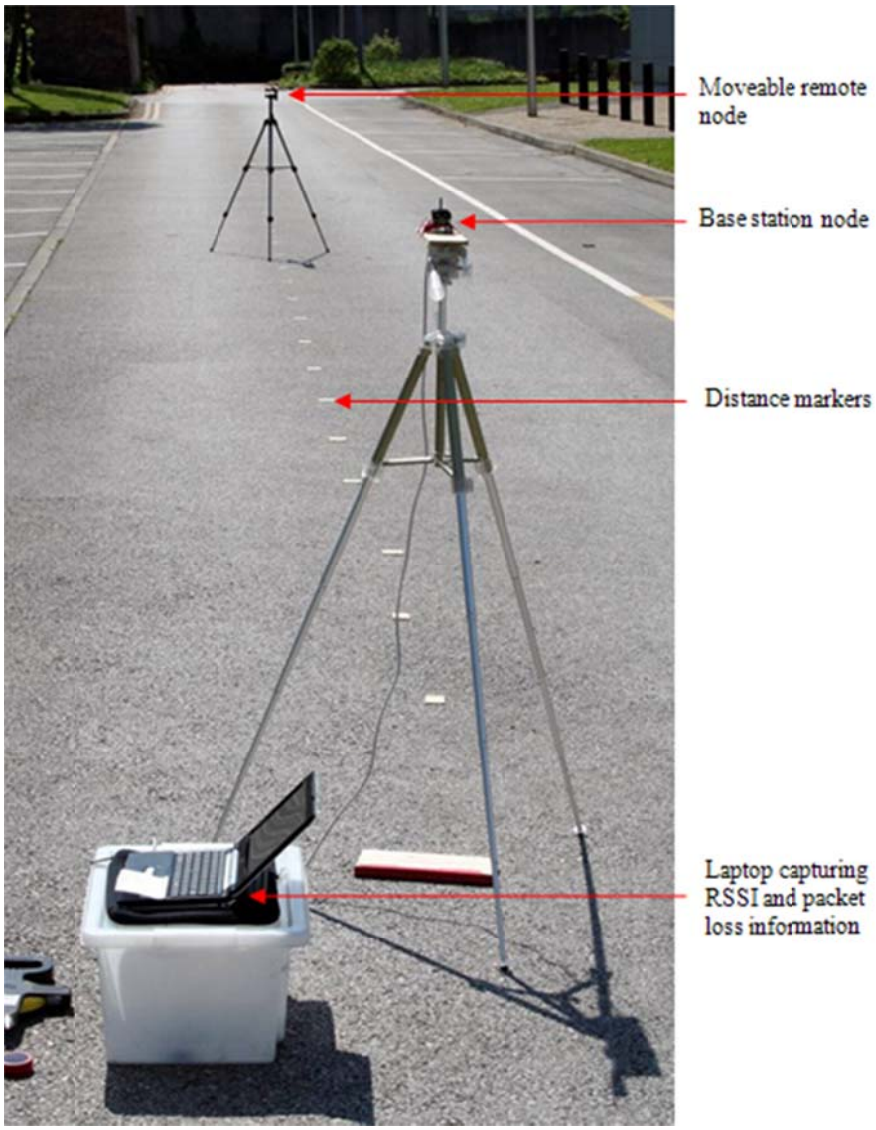

Figure 21. RSSI and packet loss measurement setup.

4.2. MEASURED RESULTS

The results obtained for the standard MicaZ monopole antenna are shown in Figures 22 and 23, whilst those for the FCPW antenna are shown in Figures 24 and 25. Each figure includes six sets of results. The associated orientation of each set of results is given in terms of the plane which is parallel to the base station monopole antenna. The orientations are relative to those shown in Figures 13. For a polarisation mismatch the base station antenna was moved from being vertical to being horizontal with respect to the Earth.

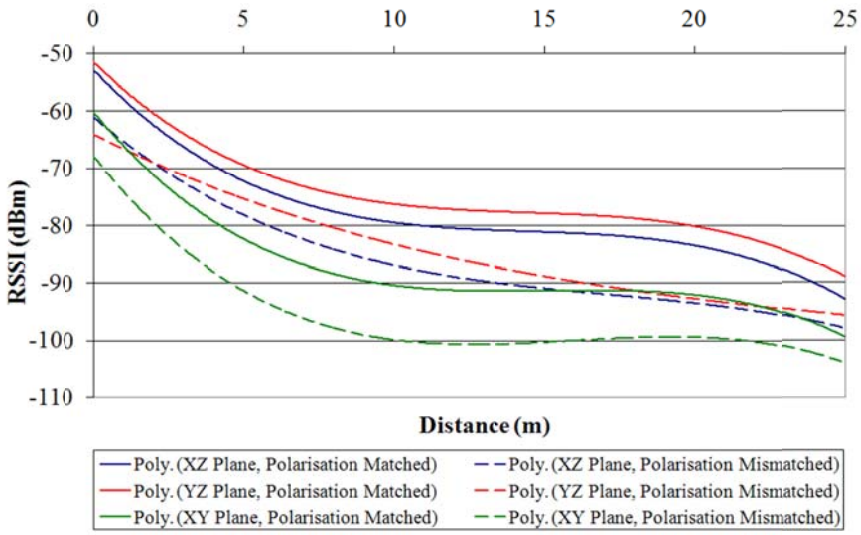

Figure 22. MicaZ monopole antenna RSSI as a function of distance.

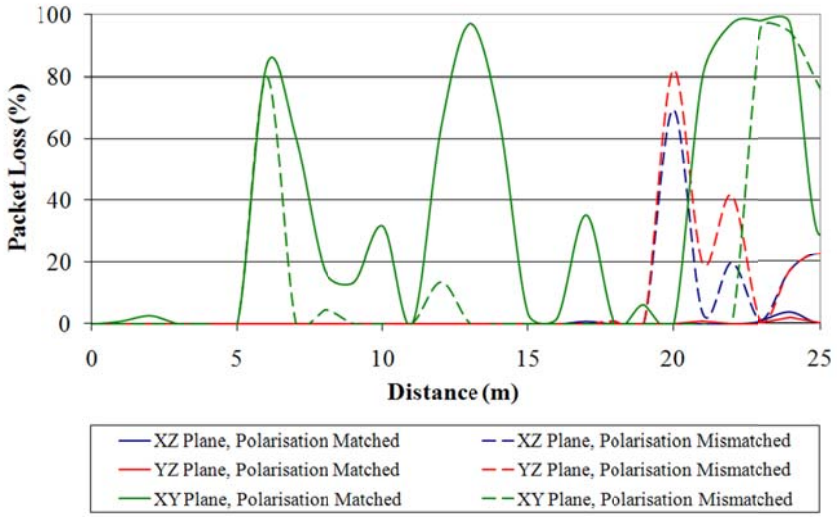

Figure 23. MicaZ monopole antenna packet loss as a function of distance.

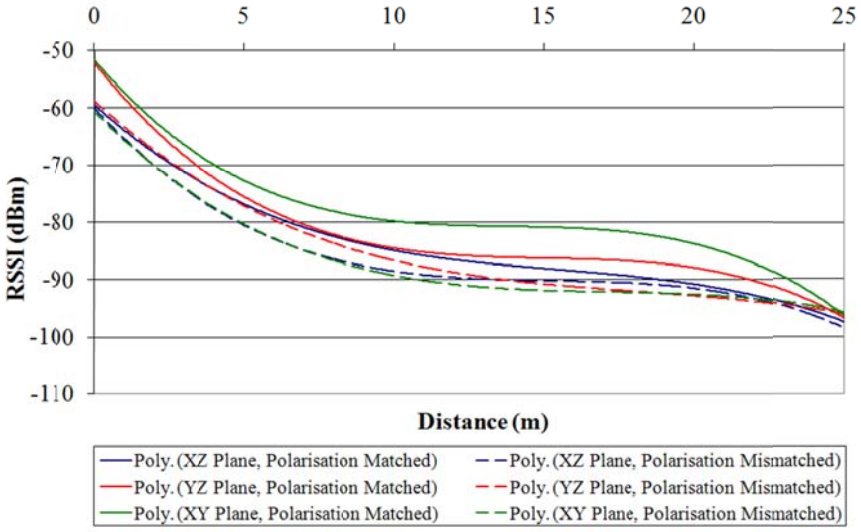

Figure 24. MicaZ FCPW antenna RSSI as a function of distance

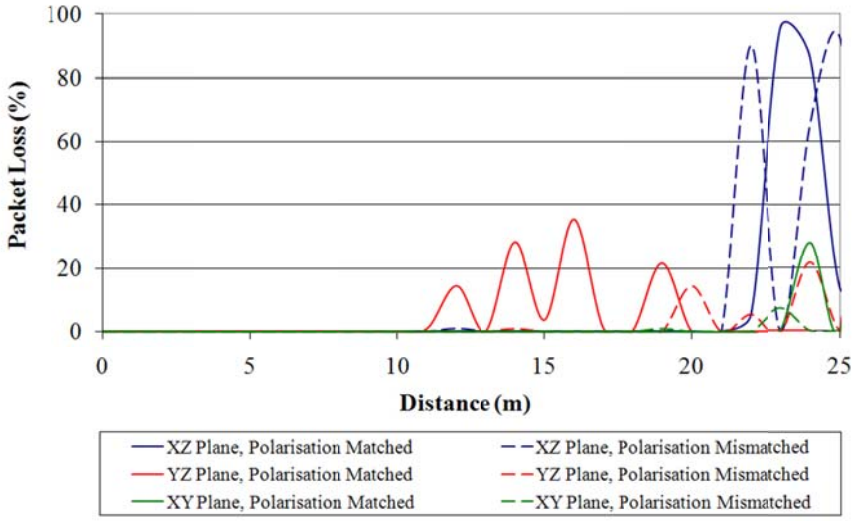

Figure 25. MicaZ FCPW antenna packet loss as a function of distance

4.3. DISCUSSION

Comparing the RSSI results (Figures 22 and 24), the monopole antenna performs best when it is vertical with respect to Earth (i.e. with the *xz* and *yz* planes) and there is no polarisation mismatch. For the FCPW antenna, the best performance is achieved when the copper face of the antenna is facing the base station (i.e. the *xy* plane) and there is no polarisation mismatch. It is notable that whilst the monopole antenna gives the highest RSSI result (*yz* plane), it displays the largest variation in results also. Comparing the results in the *yz* plane with no polarisation mismatch and those in the *xy* plane with a polarisation mismatch there is a 20-25dBm difference. Looking at the best and worst results for the FCPW, the difference is limited to a maximum of almost 10dBm.

The RSSI results do not tell the whole story however, which is why the packet loss results (Figures 23 and 25) are also included. These results show that the monopole antenna experiences heavy packet loss when it is orientated in the *xy* plane, even at a distance of just 2m. As the distance increases this packet loss varies greatly, and on numerous occasions peaks at over 50% loss. For the FCPW antenna however, packet loss does not appear to occur at all until a distance of 11m, and even then it is not as pronounced as that experienced by the monopole antenna.

It is thought that these results are due to the FCPW antenna having an elliptical polarisation, as discussed in Section 4. This is a significant finding, since it is likely that WSN nodes will be deployed in close proximity to one another in many applications, and therefore often it is short range communications (<10m) which are of most interest. These results indicate that the FCPW antenna would be far more efficient than the typical monopole in this situation. It is difficult to quantify precisely how much more efficient the FCPW antenna would be, as differing environments and data recovery mechanisms would result in differing levels of wasted energy.

Using the data present in Figures 23 and 25, we can say that 6000 data packets are transmitted between the transmitter and receiver for every 1m increment, beginning at 0m (i.e. there are 1000 packets per orientation plane, and two polarisations). Table 3 attempts to give a quantitative evaluation of how much more energy is used effectively when using the FCPW antenna in this particular scenario. The energy consumed per packet transmitted was calculated using oscilloscope measurements shown in Figure 26. This calculated figure is 6.08mW per packet, assuming average power consumption during processing and transmitting of 37.5mW and 60.5mW respectively. As one can see from Table 3, a significant amount of energy is put to more effective use by utilising the FCPW antenna in both the 0-10 and 0-25m ranges. Whilst these experiments took place outdoors in line-of-sight conditions, it is not unreasonable to expect similar performance differences in real world applications.

Table 3. Energy efficiency comparison of the monopole and FCPW antennas.

Distance	Packets transmitted	Packets lost		Energy wasted due to lost packets (J)		Increase in energy used effectively (J)
		Monopole	FCPW	Monopole	FCPW	
0-10m	72000	2946	0	17.9	0	17.9
0-25m	156000	15784	6315	95.9	38.4	57.5

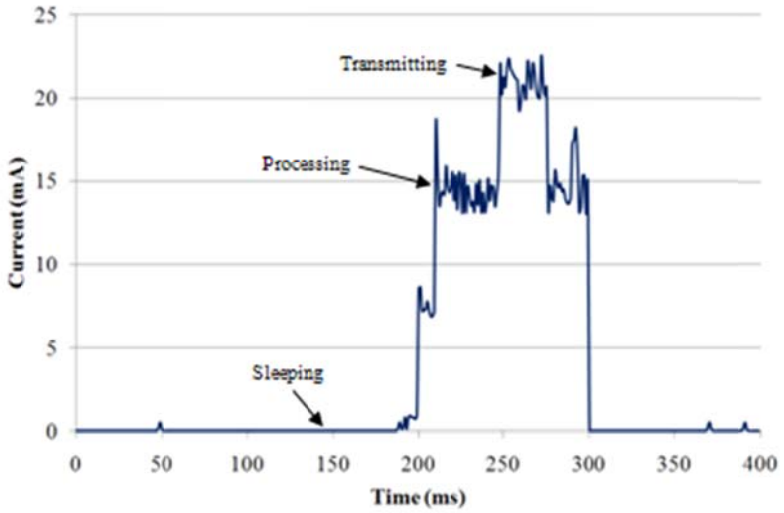

Figure 26. Measured time period and current for a single packet transmission from the MicaZ mote.

5. CONCLUSIONS

This work presents an alternative antenna design appropriate for use at 2.45GHz. It is cheap to produce and provides more than adequate bandwidth for Zigbee devices such as the Berkeley MicaZ mote whilst remaining relatively small (40mm×27.5mm×1.6mm). It also has good omni-directional characteristics which make it extremely well suited to applications where node orientation is not known and cannot be controlled. This leads to greater energy efficiency in these applications, since it means data loss is less likely. For WSNs this is an important outcome as energy constraints are often foremost in the minds of those planning sensor node deployments.

It is also noteworthy that the useable impedance bandwidth makes the FCPW antenna appropriate for use in other wireless communications standards such as IEEE802.11 and IEEE802.16 (Wi-Fi and WiMAX, respectively). The former has a similar frequency range to IEEE802.15.4 compliant devices (such as the Berkeley MicaZ mote), whilst the later operates at 2.3, 2.5 and 3.5GHz.

6. REFERENCES

[1] Crossbow. (2004, 6 April 2010). MPR/MIB Users Manual. Available: http://www.xbow.com/

[2] A. Mason, *et al.*, "Inventory Management in The Packaged Gas Industry Using Wireless Sensor Networks," in *Advances in Wireless Sensors and Sensor Networks*. vol. 64, Subhas Chandra Mukhopadhyay and H. Leung, Eds., 1st ed: Springer, 2010, pp. 75-100.

[3] A. Mason, *et al.*, "Asset Tracking: Beyond RFID," presented at the 7th Annual Postgraduate Symposium on the Convergence of Telecommunications (PGNET), Liverpool John Moores University, Liverpool, UK, 2006.

[4] A. Mason, "Wireless Sensor Networks and their Industrial Applications," PhD, General Engineering Research Institute, Liverpool John Moores University, Liverpool, 2008.

[5] C. Balanis, "Microstrip Antennas," in *Antennas: Theory, Analysis and Design* 2nd ed: Wiley, 1996, pp. 727-730.

[6] F. Ulaby, "Quarter wave monopole antenna," in *Fundamentals of Applied Electromagnetics*, ed: Prentice Hall, 1999, p. 358.

[7] C. Balanis, "Loop Antennas," in *Antennas: Theory, Analysis and Design* 2nd ed: Wiley, 1996, p. 203.

[8] L. Blake, "Radiation Resistance and Efficiency," in *Antennas*, ed: John Wiley & Sons, 1966, pp. 138-139.

[9] C. Balanis, "Bandwidth," in *Antennas: Theory, Analysis and Design* 2nd ed: Wiley, 1996, pp. 63-64.

[10] R. Garg, *et al.*, "Broadbanding of Microstrip Antennas," in *Microstrip Antenna Design Handbook*, ed: Artech House, 2000, pp. 534-535.

[11] C. Balanis, "Long Wire Antenna Polarisation," in *Antennas: Theory, Analysis and Design* 2nd ed: Wiley, 1996, p. 496.

[12] K. Nithisopa, *et al.*, "Design CPW Fed Slot Antenna for Wideband Applications," *Piers Online,* vol. 3, pp. 1124-1127, 2007.

[13] R. Garg, *et al.*, "Effects of Finite Size Ground Plane," in *Microstrip Antenna Design Handbook*, ed: Artech House, 2000, pp. 293-296.

[14] Ansoft. Probe Feed Patch Antenna Example. *HFSS Users Guide*. Available: www.ansoft.com/

[15] Ansoft. *Ansoft HFSS*. Available: www.ansoft.com/products/hf/hfss

[16] Ansoft. (2005, 22/05/2008). Port tutorial series: Coplanar waveguide (CPW). *HFSS v8 Training*. Available: http://web.doe.carleton.ca/~mmariani/Thesis/port_tutorial_CPW.ppt

[17] J. Carr, "Transmission Lines Characteristic Impedance," in *Practical Antenna Handbook*, 4th ed: Tab Books, 2001, p. 67.

[18] C. Balanis, "Microstrip Antennas: Patch Antenna Example," in *Antennas: Theory, Analysis and Design* 2nd ed: Wiley, 1996, pp. 727-730.

[19] J. Kraus and R. Marhefka, "Folded Dipole Antennas," in *Antennas for All Applications*, ed: McGraw Hill Science, 2002, pp. 593-597.

[20] J. Kraus and R. Marhefka, "Anechoic Chambers and Absorbing Materials," in *Antennas for All Applications*, ed: McGraw Hill Science, 2002, pp. 841-844.

[21] F. Ulaby, "Plane Wave Propagation in Lossy Media," in *Fundamentals of Applied Electromagnetics*, ed: Prentice Hall, 1999, pp. 277-279.

[22] L. Blake, "Interference," in *Antennas*, ed: John Wiley & Sons, 1966, pp. 26-27.

[23] J. Carr, "Fading Mechanisms," in *Practical Antenna Handbook*, 4th ed: Tab Books, 2001, p. 35.

[24] S. Basagni, *et al.*, "Multipath Fading and Shadowing," in *Mobile Adhoc Networking*, ed: Wiley-Blackwell, 2004, pp. 235-236.
[25] C. Balanis, "Horn Antennas," in *Antennas: Theory, Analysis and Design* 2nd ed: Wiley, 1996, pp. 651-711.
[26] C. Balanis, "Field Regions," in *Antennas: Theory, Analysis and Design* 2nd ed: Wiley, 1996, p. 33.
[27] L. Blake, "Waveguides," in *Antennas*, ed: John Wiley & Sons, 1966, p. 94.
[28] C. Balanis, *Antennas: Theory, Analysis and Design* 2nd ed.: Wiley, 1996.
[29] J. Kraus and R. Marhefka, *Antennas for All Applications*: McGraw Hill Science, 2002.